

## CHAPTER IV

### RESULTS AND DISCUSSION

In 2013, Wongpraphairoat N. and co-workers studied the effects of supports in Cu/ZnO based catalysts. The catalysts were prepared by incipient wetness impregnation over alumina ( $\text{Al}_2\text{O}_3$ ), amorphous silica-alumina (ASA), magnesium oxide (MgO), and hydrotalcite ( $\text{Mg}_6\text{Al}_2\text{CO}_3(\text{OH})_{16}\cdot 4(\text{H}_2\text{O})$ ). Among the four catalysts, CuZnO/ $\text{Al}_2\text{O}_3$  showed the highest catalytic activity in dehydroxylation of glycerol to propylene glycol. However, CuZnO/MgO catalyst exhibited the highest performance in terms of stability. In order to further improve the catalysts, CuZnO loaded on MgO– $\text{Al}_2\text{O}_3$  mixed oxide supports were studied in this work.

#### 4.1 Catalytic Characterization

Textual properties of the supports and the catalysts are provided in Table 4.1. It is noticeable that the surface area of mixed oxide supports decreased with increasing magnesium oxide contents. In addition, surface area and pore volume of all catalysts were lower than those of the corresponding supports. This loss of surface area and pore volume might be due to the high amount of metal loading which block the pore of the supports. Nevertheless, the pore diameter remained invariant, indicating that the loaded metal might partially block the pores.

X-ray fluorescence spectrometer (XRF) was employed to examine the actual metal loadings of the Cu, Zn, Mg, and Al on the catalysts. The XRF results are summarized in Table 4.2. The actual compositions of MgO and  $\text{Al}_2\text{O}_3$  in mixed oxide supports are shown in Appendix A. The results indicated that the amounts of Cu, Zn, and Al were lower than the expected metal loadings while the amount of Mg become higher compared to expected metal loading in catalysts. This could be due to metal precursor impurity and less efficiently of Cu and Zn impregnation in the catalysts. Moreover, the low efficiency of fluorescence detection of Mg and Al which were light elements might cause the discrepancy of Mg and Al actual loadings, as reported by Weber *et al.* (1993).

**Table 4.1** BET surface area, pore volume, and pore size diameter of the supports and the catalysts

Catalysts	Surface area (m <sup>2</sup> /g)		Pore volume (mL/g)		Pore diameter (nm)	
	Support	Catalyst	Support	Catalyst	Support	Catalyst
CuZnO/Al <sub>2</sub> O <sub>3</sub>	290	88	0.48	0.16	6.65	7.45
CuZnO/MgO(5)-Al <sub>2</sub> O <sub>3</sub> (95)	278	73	0.67	0.21	9.63	11.19
CuZnO/MgO(10)-Al <sub>2</sub> O <sub>3</sub> (90)	188	63	0.55	0.21	13.73	11.62
CuZnO/MgO(15)-Al <sub>2</sub> O <sub>3</sub> (85)	182	54	0.49	0.19	10.81	13.99
CuZnO/MgO(20)-Al <sub>2</sub> O <sub>3</sub> (80)	167	51	0.42	0.15	10.10	11.92
CuZnO/MgO(30)-Al <sub>2</sub> O <sub>3</sub> (70)	157	45	0.30	0.14	9.64	12.01
CuZnO/MgO	142	6	0.38	0.12	10.78	9.01

**Table 4.2** The actual metal loading of the catalysts

<b>Catalysts</b>	<b>Cu (wt.%)</b>	<b>Zn (wt.%)</b>	<b>Mg (wt.%)</b>	<b>Al (wt.%)</b>
CuZnO/Al <sub>2</sub> O <sub>3</sub>	9.01	36.80	-	22.50
CuZnO/MgO(5)-Al <sub>2</sub> O <sub>3</sub> (95)	8.54	34.90	3.33	21.30
CuZnO/MgO(10)-Al <sub>2</sub> O <sub>3</sub> (90)	8.04	32.20	6.08	21.00
CuZnO/MgO(15)-Al <sub>2</sub> O <sub>3</sub> (85)	8.15	32.70	8.53	18.40
CuZnO/MgO(20)-Al <sub>2</sub> O <sub>3</sub> (80)	8.18	33.10	11.00	16.00
CuZnO/MgO(30)-Al <sub>2</sub> O <sub>3</sub> (70)	8.00	31.90	15.40	13.00
CuZnO/MgO	7.39	28.80	32.80	-

Figure 4.1 shows the XRD patterns of the prepared CuZnO-based catalysts with different Mg and Al contents in mixed oxide supports. The XRD patterns of all catalysts were quite similar, consisting of ZnO phases and CuO phase. In contrast, Cu<sub>2</sub>O phase, MgO phase and MgZnO phase ( $2\theta$  of 43.0°, 62.4°, 78.7°) were found only in CuZnO/MgO. It is interesting to note that the small intensity of CuO ( $2\theta = 35.6^\circ, 38.8^\circ$ ) peaks have been observed in the catalysts, confirming that Cu are well dispersed on the surface of the supports (Gurram *et al.*, 1998).

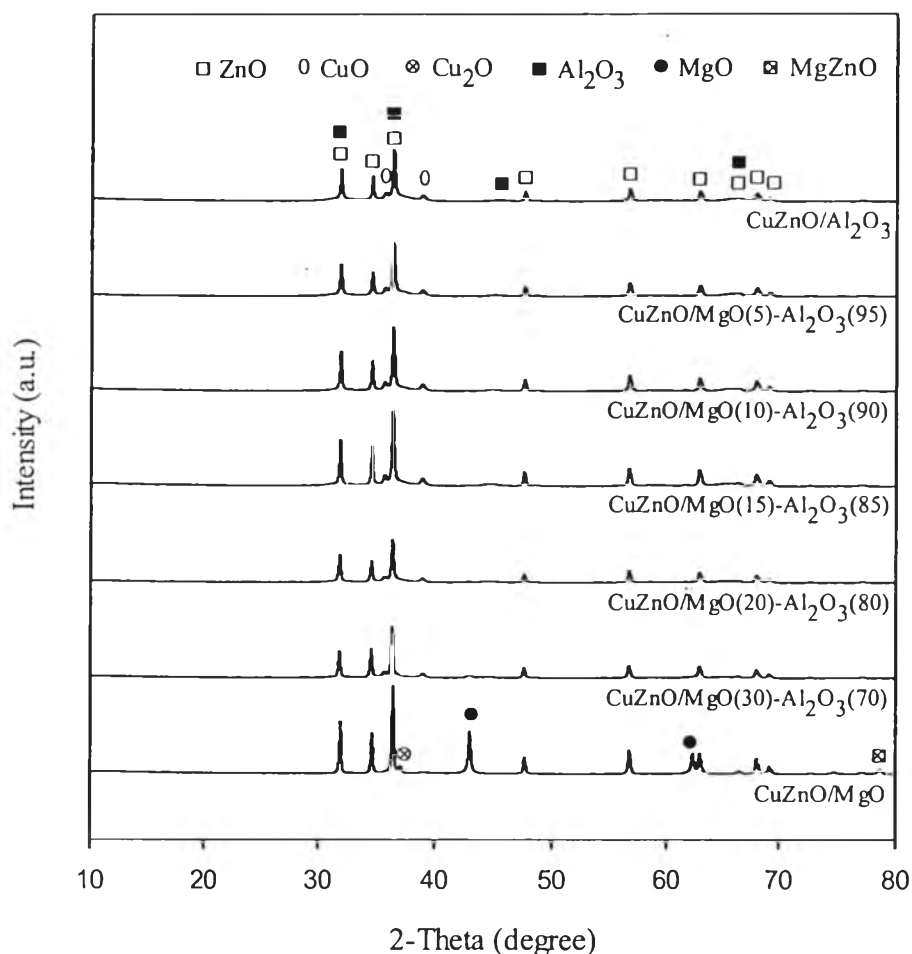


**Figure 4.1** XRD patterns of the impregnated CuZnO-based catalysts with different MgO and Al<sub>2</sub>O<sub>3</sub> contents in mixed oxide supports.

The reduction behaviors of the catalysts were studied using hydrogen-temperature programmed reduction (H<sub>2</sub>-TPR) technique. The H<sub>2</sub>-TPR profiles of the catalysts are shown in Figure 4.2. The CuZnO/Al<sub>2</sub>O<sub>3</sub> showed a symmetric reduction peak at the lowest temperature (237 °C), indicating the reduction peak of homogeneous size distribution and highly dispersion of copper oxide clusters on the catalysts. The reduction peaks of CuZnO/MgO-Al<sub>2</sub>O<sub>3</sub> shifted to higher temperature with broader peaks as increased MgO contents in the supports. The higher reduction temperature assigned to the reduction of Cu metals having interaction with supports (Kee *et al.*, 2008). In case of the reduction peak of CuZnO/MgO(30)-Al<sub>2</sub>O<sub>3</sub>(70), the peak shifts toward the lower temperature (260 °C) with a shoulder at 295 °C. This might be due to the agglomeration of Cu species decreased Cu surface area (Kee *et al.*, 2008).

In case of CuZnO/MgO catalyst, the H<sub>2</sub>-TPR profile showed the peak at 257 °C with a small shoulder at 280 °C, indicating the presence of two different copper oxide species. Those peaks are assigned to the reduction of CuO (Cu<sup>2+</sup>) and Cu<sub>2</sub>O (Cu<sup>1+</sup>) species, respectively (Delahay *et al.*, 1997). In addition, the hydrogen consumption of CuZnO/MgO was much less than those of other catalysts. This illustrated that the lower amount of CuO species was reduced. Furthermore, the X-ray photoelectron spectroscopy (XPS) technique was employed to confirm the effect of metal support interaction as shown in Appendix B.

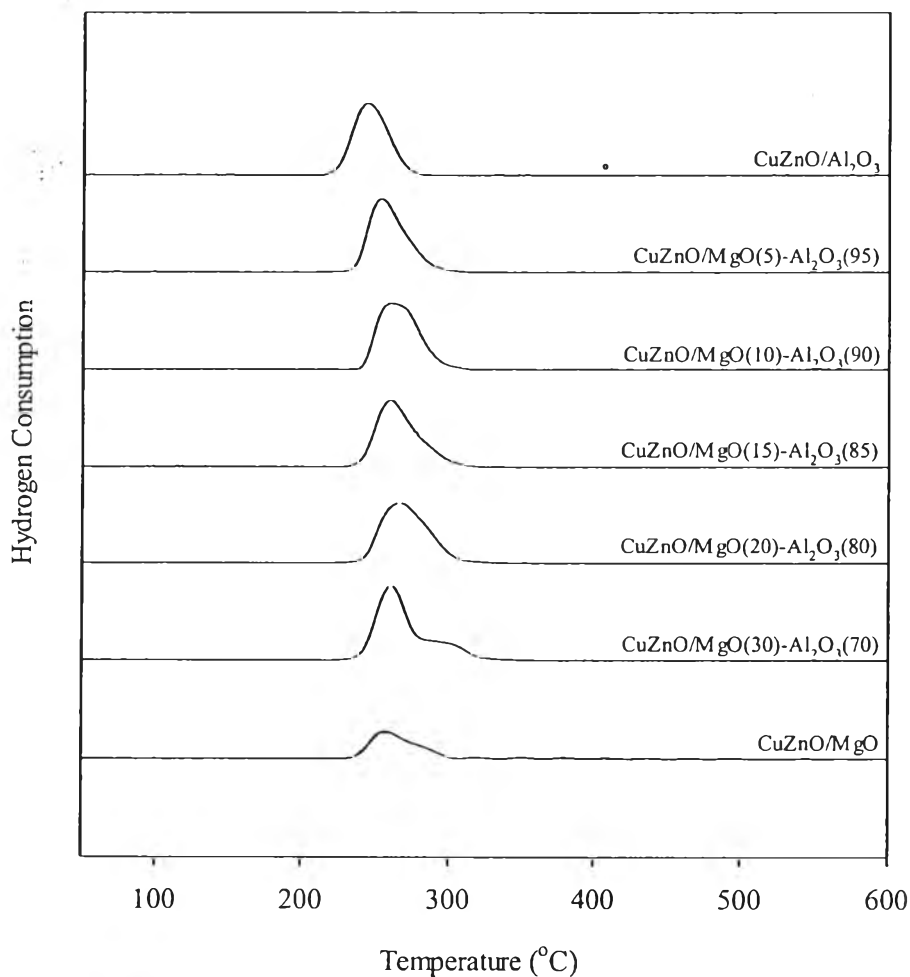


**Figure 4.2** Temperature programmed reduction (TPR) profiles of the CuZnO-based catalysts with different MgO and Al<sub>2</sub>O<sub>3</sub> contents in mixed oxide supports.

The acid properties of CuZnO/Al<sub>2</sub>O<sub>3</sub> and CuZnO/MgO(15)-Al<sub>2</sub>O<sub>3</sub>(85) catalysts were also determined by NH<sub>3</sub>-TPD. The NH<sub>3</sub>-TPD profiles of CuZnO/Al<sub>2</sub>O<sub>3</sub> and CuZnO/MgO(15)-Al<sub>2</sub>O<sub>3</sub>(85) are shown in Figure 4.3. Generally, the quantities of weak, medium, and strong acid sites were found at 120-200 °C, between 200-400 °C and above 400 °C, respectively. The CuZnO/Al<sub>2</sub>O<sub>3</sub> and CuZnO/MgO(15)-Al<sub>2</sub>O<sub>3</sub>(85) exhibited the similar desorption peaks which are the weak acid site peak and medium acid site peak. However, the CuZnO/MgO(15)-Al<sub>2</sub>O<sub>3</sub>(85) showed the lower intensity of desorption peak compared to CuZnO/Al<sub>2</sub>O<sub>3</sub>,

indicating the weaker acid site catalyst. Moreover, CuZnO/Al<sub>2</sub>O<sub>3</sub> showed the higher total amount of acidity compared to the CuZnO/MgO(15)-Al<sub>2</sub>O<sub>3</sub>(85) as observed in Table 4.3. This might be due to the addition of MgO to alumina support affected the total acid sites of catalysts (Abello, *et al.* 1998).

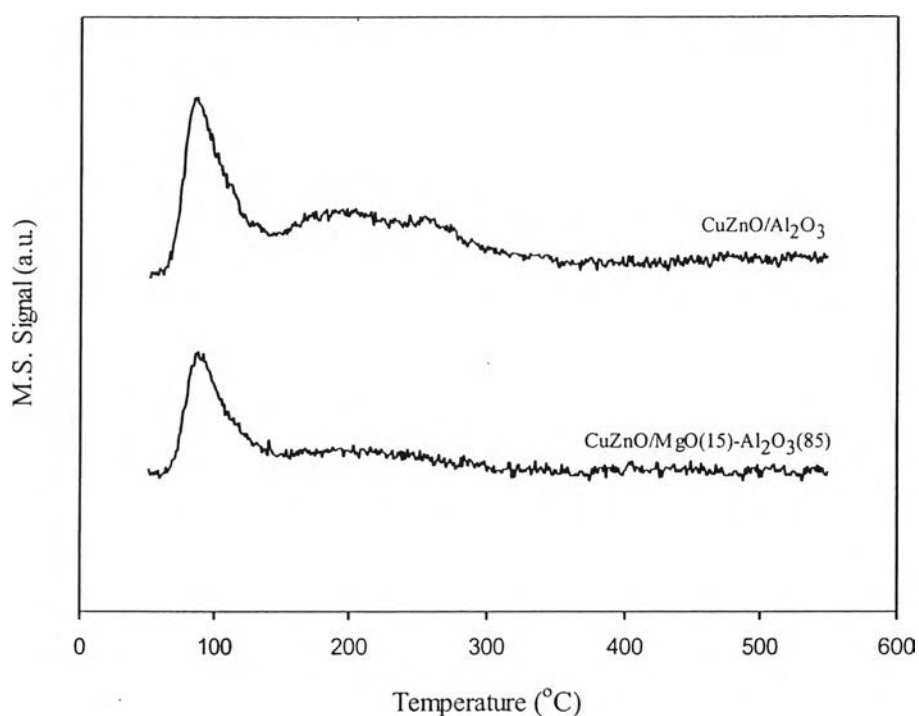


**Figure 4.3** Ammonia-TPD (NH<sub>3</sub>-TPD) profiles of CuZnO/Al<sub>2</sub>O<sub>3</sub> and CuZnO/MgO(15)-Al<sub>2</sub>O<sub>3</sub>(85) catalysts.

**Table 4.3** Acidic properties of CuZnO/Al<sub>2</sub>O<sub>3</sub> and CuZnO/MgO(15)-Al<sub>2</sub>O<sub>3</sub>(85) catalysts

Catalysts	Acid amount ( $\mu\text{mol NH}_3/\text{g}_{\text{cat}}$ )		
	Weak	Medium	Total
CuZnO/Al <sub>2</sub> O <sub>3</sub>	66	107	173
CuZnO/MgO(15)-Al <sub>2</sub> O <sub>3</sub> (85)	38	27	65

## 4.2 Catalytic Activity Testing

### 4.2.1 Effect of MgO and Al<sub>2</sub>O<sub>3</sub> Contents in Mixed Oxide Supports

The effects of MgO and Al<sub>2</sub>O<sub>3</sub> contents in mixed oxide supports to the catalytic activity were investigated over different catalysts (CuZnO/Al<sub>2</sub>O<sub>3</sub>, CuZnO/MgO(5)-Al<sub>2</sub>O<sub>3</sub>(95), CuZnO/MgO(10)-Al<sub>2</sub>O<sub>3</sub>(90), CuZnO/MgO(15)-Al<sub>2</sub>O<sub>3</sub>(85), CuZnO/MgO(20)-Al<sub>2</sub>O<sub>3</sub>(80), CuZnO/MgO(30)-Al<sub>2</sub>O<sub>3</sub>(70), and CuZnO/MgO). The plots of glycerol conversion, propylene glycol (PG) selectivity, acetol selectivity and ethylene glycol (EG) selectivity as a function of time on stream are illustrated in Figure 4.4. The results showed that CuZnO/Al<sub>2</sub>O<sub>3</sub> exhibited the highest catalytic activity, followed by CuZnO/MgO(15)-Al<sub>2</sub>O<sub>3</sub>(85), CuZnO/MgO(10)-Al<sub>2</sub>O<sub>3</sub>(90), CuZnO/MgO(5)-Al<sub>2</sub>O<sub>3</sub>(95), CuZnO/MgO(20)-Al<sub>2</sub>O<sub>3</sub>(80), CuZnO/MgO(30)-Al<sub>2</sub>O<sub>3</sub>(70), and CuZnO/MgO, respectively. This could be due to the higher surface area of CuZnO/Al<sub>2</sub>O<sub>3</sub> compared to the others. However, the glycerol conversion over CuZnO/Al<sub>2</sub>O<sub>3</sub> was continuously dropped in a longer reaction time, while the CuZnO/MgO(15)-Al<sub>2</sub>O<sub>3</sub>(85) gave the invariable conversion. This evidence indicated that the mixed oxide supports with appropriate composition could improve the stability of the catalyst.

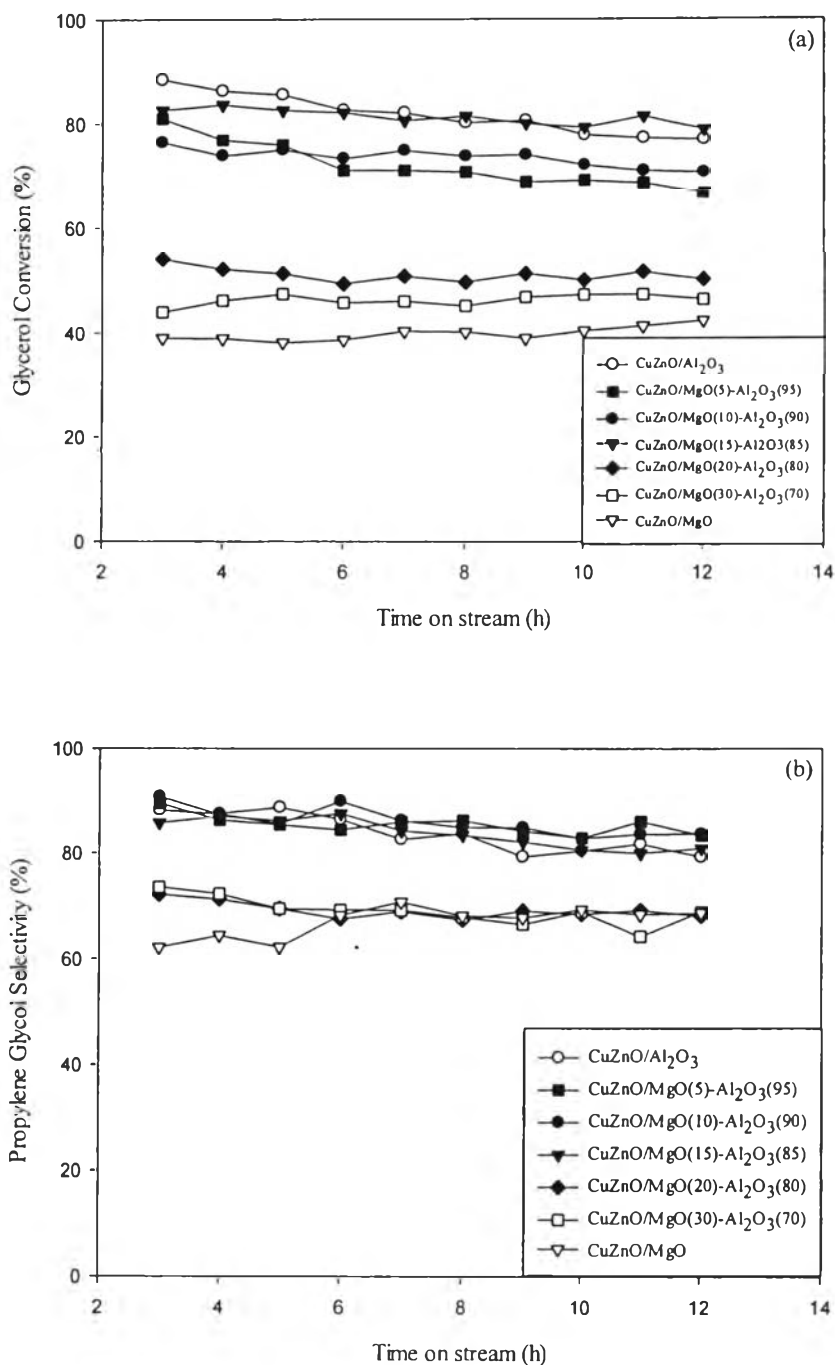


**Figure 4.4** Plots of (a) glycerol conversion, (b) PG selectivity, (c) acetol selectivity, and (d) EG selectivity as a function of time on stream over the CuZnO-based catalysts with different MgO and Al<sub>2</sub>O<sub>3</sub> contents in mixed oxide supports (Reaction conditions: 80 wt.% glycerol feed, 250 °C, 500 psig, H<sub>2</sub>:glycerol = 4:1, and WHSV = 3.77 h<sup>-1</sup>).

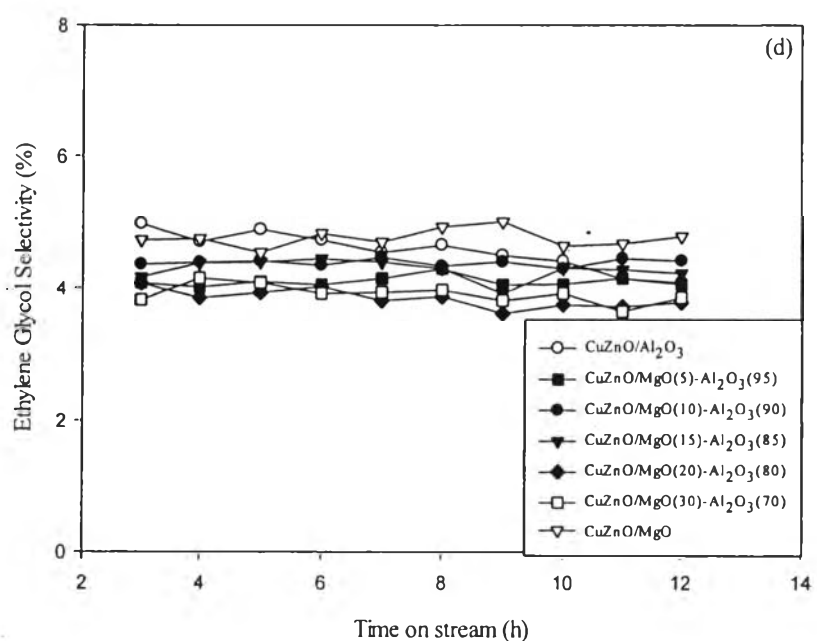
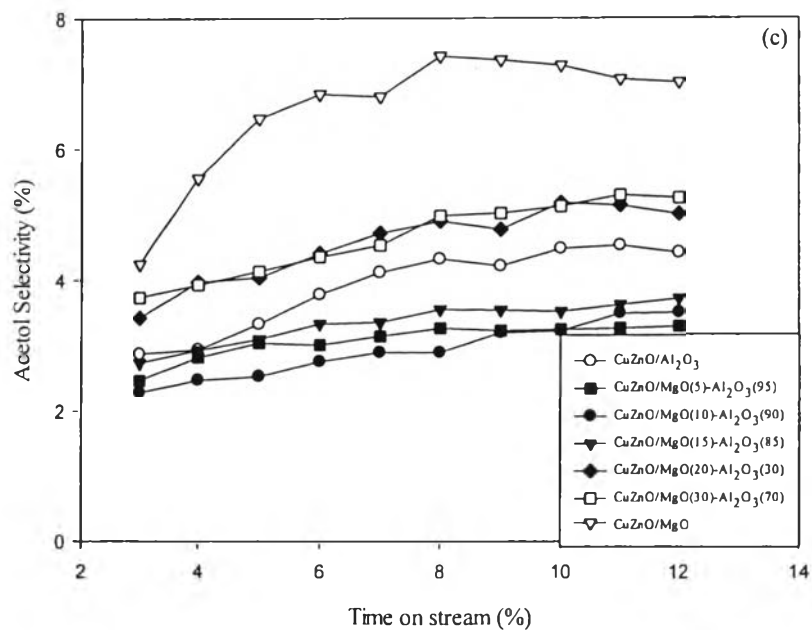


**Figure 4.4 (cont.)** Plots of (a) glycerol conversion, (b) PG selectivity, (c) acetol selectivity, and (d) EG selectivity as a function of time on stream over the CuZnO-based catalysts with different MgO and Al<sub>2</sub>O<sub>3</sub> contents in mixed oxide supports (Reaction conditions: 80 wt.% glycerol feed, 250 °C, 500 psig, H<sub>2</sub>:glycerol = 4:1, and WHSV = 3.77 h<sup>-1</sup>).

From Figures 4.4 (b) and (c), the propylene glycol selectivity was slightly decreased while the acetol selectivity increased. These results were in agreement with the mechanism proposed by Dasari *et al.* (2005). As shown in Figure 4.5, glycerol was dehydrated to acetol at the first step and then acetol was hydrogenated to propylene glycol. The results also indicated the deactivation of hydrogenation sites simultaneously. Furthermore, another by-product like ethylene glycol was formed by another reaction route, as proposed by Feng *et al.* (2008) (Fig. 2.12).

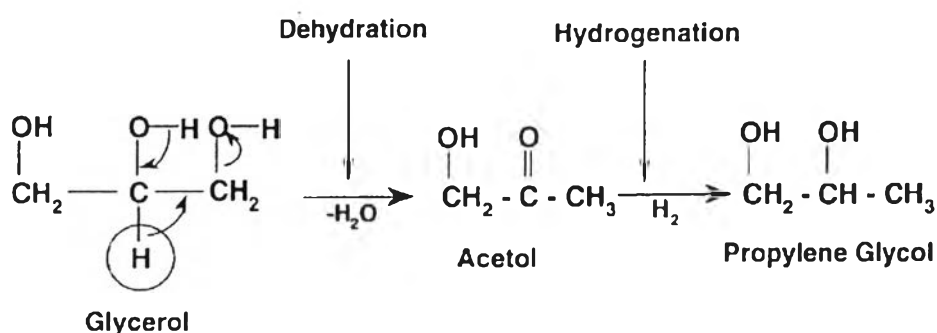


**Figure 4.5** The glycerol conversion mechanism (Dasari *et al.*, 2005).

Temperature programmed oxidation (TPO) was used to determine the nature and amounts of coke deposited on spent catalysts. As shown in Figure 4.6. It was found that the spent CuZnO/MgO contained the highest amount of coke (28.77 wt.%) followed by CuZnO/MgO(30)-Al<sub>2</sub>O<sub>3</sub>(70) (15.81 wt.%), CuZnO/MgO(20)-Al<sub>2</sub>O<sub>3</sub>(80) (11.67 wt.%), CuZnO/MgO(5)-Al<sub>2</sub>O<sub>3</sub>(95) (6.93 wt.%), CuZnO/Al<sub>2</sub>O<sub>3</sub> (4.52 wt.%), CuZnO/MgO(10)-Al<sub>2</sub>O<sub>3</sub>(90) (3.94 wt.%) and CuZnO/MgO(15)-Al<sub>2</sub>O<sub>3</sub>(85) (3.89 wt.%), respectively. This coke may be formed by undesired polymerization of unsaturated intermediates (Ertl *et al.*, 2008). In addition, coke deposition might poison the active site of the catalyst, which led to lower catalytic activity. This result is in agreement with the continued declining in catalytic activities of CuZnO/Al<sub>2</sub>O<sub>3</sub> and CuZnO/MgO(5)-Al<sub>2</sub>O<sub>3</sub>(95). This might be due to the stronger acid sites of CuZnO/Al<sub>2</sub>O<sub>3</sub> led to expedite the dehydration step of the reaction, resulting in the formation of excess amounts of acetol intermediate. So the

acetol would form other by-products and adsorbed on the surface of the catalyst led to increase the coke formation and lower catalytic stability. In addition, self-polymerization of glycerol to the heavy by-products was usually observed in acid catalysts and these by-products could block the pores of the catalysts resulted in the catalyst deactivation as reported by Oudar *et al.* (1985). However, CuZnO/MgO exhibited high stability in longer reaction time, although it had the highest amount of deposited coke. This is probably due to the considerably increasing of coke formation at the beginning of reaction (Wongpraphairoat, N., 2013).

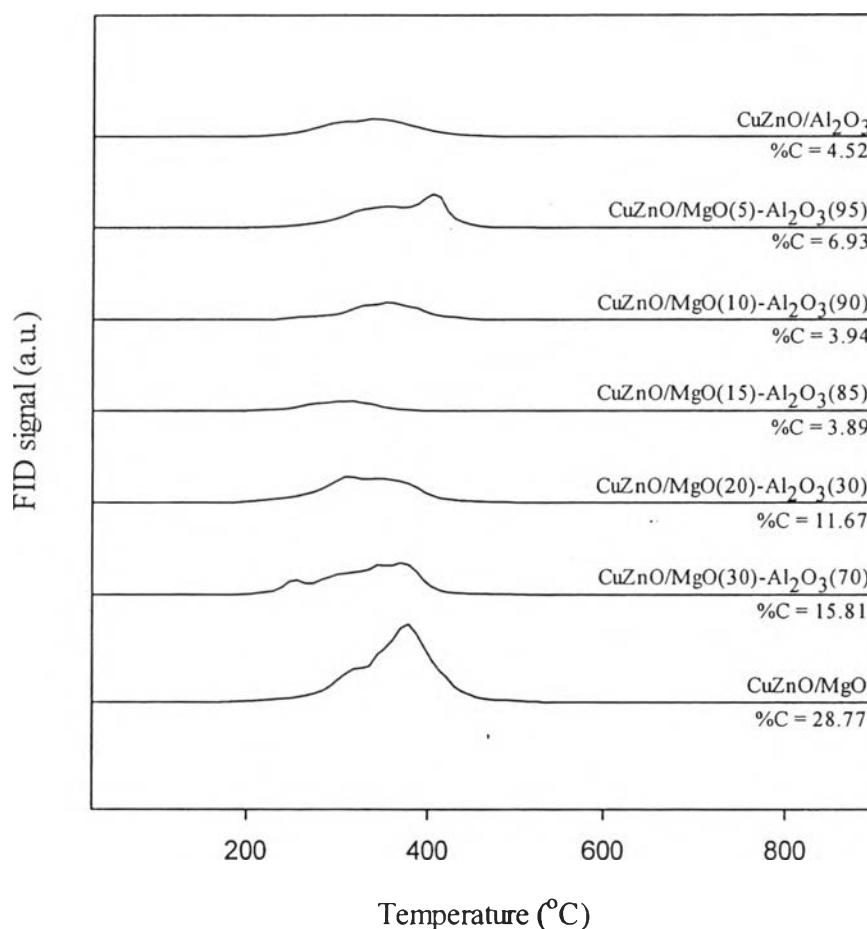


**Figure 4.6** Temperature programmed oxidation (TPO) profiles of the spent CuZnO-based catalysts with different MgO and Al<sub>2</sub>O<sub>3</sub> proportions in mixed oxide supports after 12 h TOS. (Reaction conditions: 80 wt.% glycerol feed, 250 °C, 500 psig, H<sub>2</sub>:glycerol = 4:1, and WHSV = 3.77 h<sup>-1</sup>).

Agreed with the catalytic activity testing results, CuZnO/MgO(15)-Al<sub>2</sub>O<sub>3</sub>(85) provided the high catalytic activity and stability due to much lower coke formation compared to the others. These results indicated that the addition of MgO improved the strong metal support interaction, resulting in well dispersion of metal particles and high coke resistance, as reported by Kee *et al.* (2008). Nevertheless, in case of CuZnO/MgO(20)-Al<sub>2</sub>O<sub>3</sub>(80) and CuZnO/MgO(30)-Al<sub>2</sub>O<sub>3</sub>(70) catalysts, excess MgO loading decreased the surface area of catalysts, resulting in agglomeration of Cu particles and lower catalytic activity.

#### 4.2.2 Effect of Yellow Grade Glycerol Feedstock

Generally, the by-product glycerol from biodiesel production are divided into four grades ranging, crude glycerol, technical grade glycerol, yellow grade glycerol, and refined glycerol. In economic point of view, the price of yellow grade glycerol is lower than refined glycerol, which is more promising to use as a feedstock. Therefore, the yellow grade glycerol was used as feed for dehydroxylation of glycerol to propylene glycol over the two highest performance catalysts (CuZnO/Al<sub>2</sub>O<sub>3</sub> and CuZnO/MgO(15)-Al<sub>2</sub>O<sub>3</sub>(85))

The effect of feedstocks, refined glycerol and yellow grade glycerol, to the catalytic activity of CuZnO/Al<sub>2</sub>O<sub>3</sub> and CuZnO/MgO(15)-Al<sub>2</sub>O<sub>3</sub>(85) catalysts are shown in Figure 4.7. As expected, the presence of impurities in yellow grade glycerol resulted in lower catalytic activity of the catalysts. Nevertheless, CuZnO/MgO(15)-Al<sub>2</sub>O<sub>3</sub>(85) exhibited the higher glycerol conversion and propylene glycol selectivity as compared to CuZnO/Al<sub>2</sub>O<sub>3</sub>. It was noticed that the catalytic activity of CuZnO/Al<sub>2</sub>O<sub>3</sub> is high at the beginning, and then dropped considerably with time on stream. The results indicated that the higher concentration of impurities (MONG) tended to poison the active site of the catalysts, resulting in lower catalytic activity and stability. As the conversion decreased, the propylene glycol selectivity decreased with increasing of acetol selectivity. These agree well with the mechanism proposed by Dasari *et al.* (2005) (Fig. 4.5).

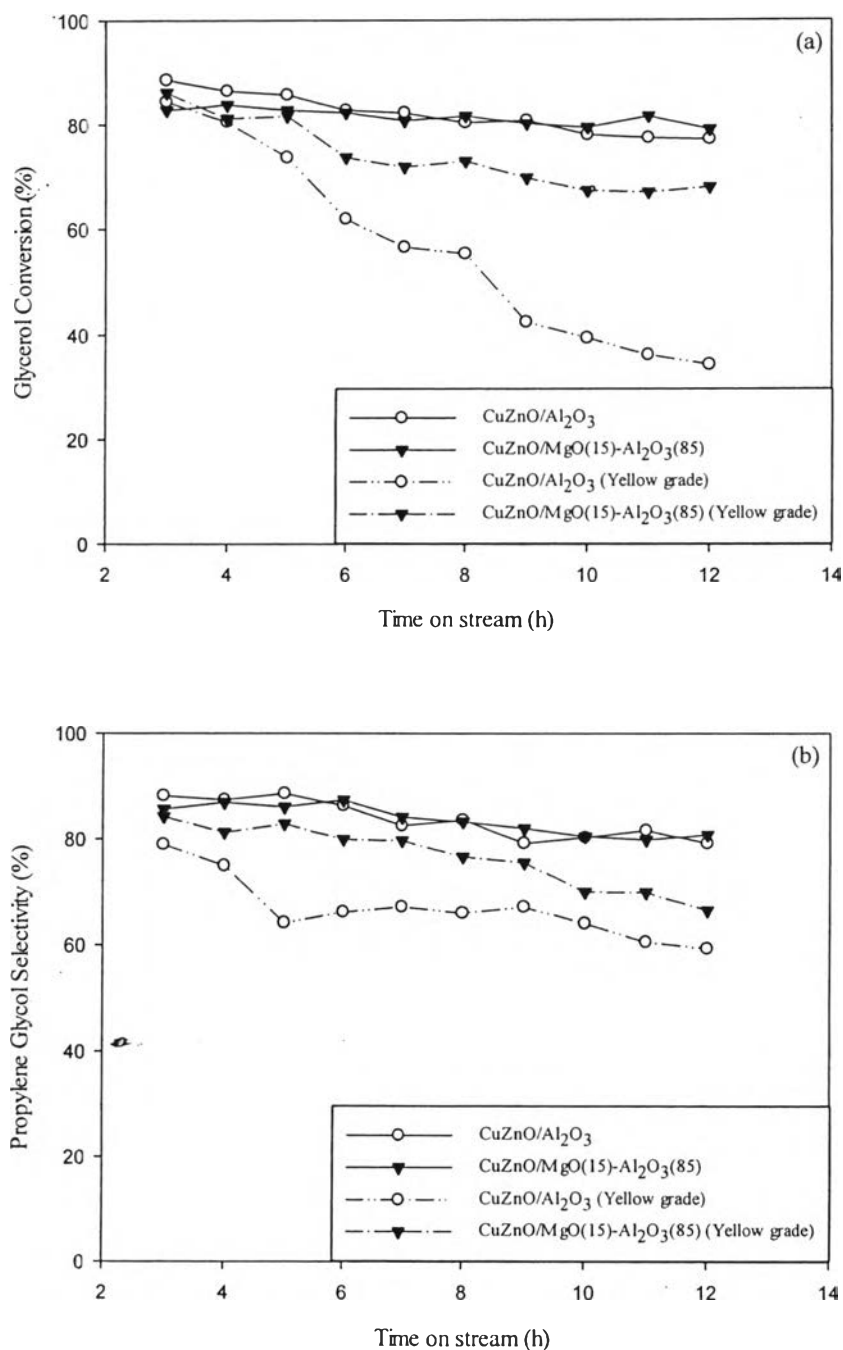


**Figure 4.7** Plots of (a) glycerol conversion, (b) PG selectivity, (c) acetol selectivity, and (d) EG selectivity as a function of time on stream over CuZnO/Al<sub>2</sub>O<sub>3</sub> and CuZnO/MgO(15)-Al<sub>2</sub>O<sub>3</sub>(85) catalysts in yellow grade glycerol feedstock (Reaction conditions: 80 wt.% glycerol feed, 250 °C, 500 psig, H<sub>2</sub>:glycerol = 4:1, and WHSV = 3.77 h<sup>-1</sup>).

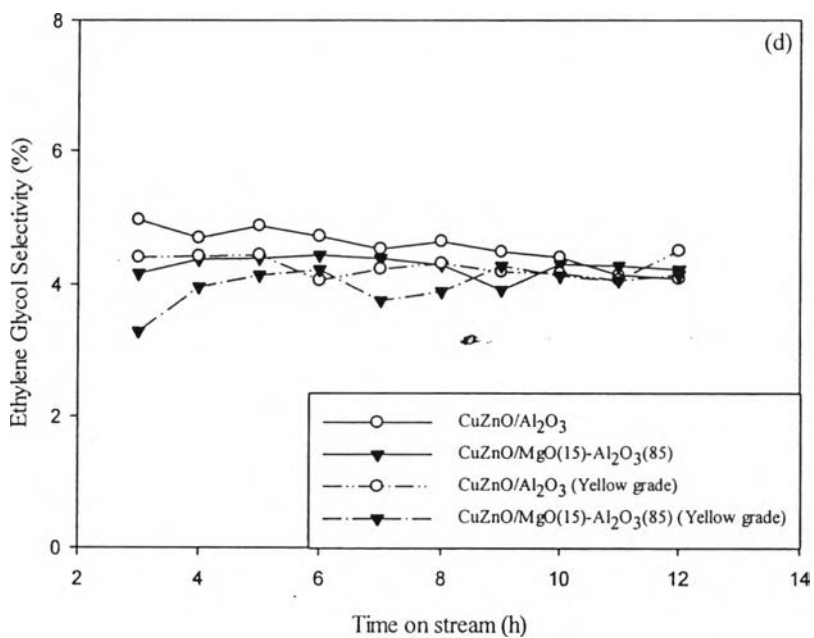
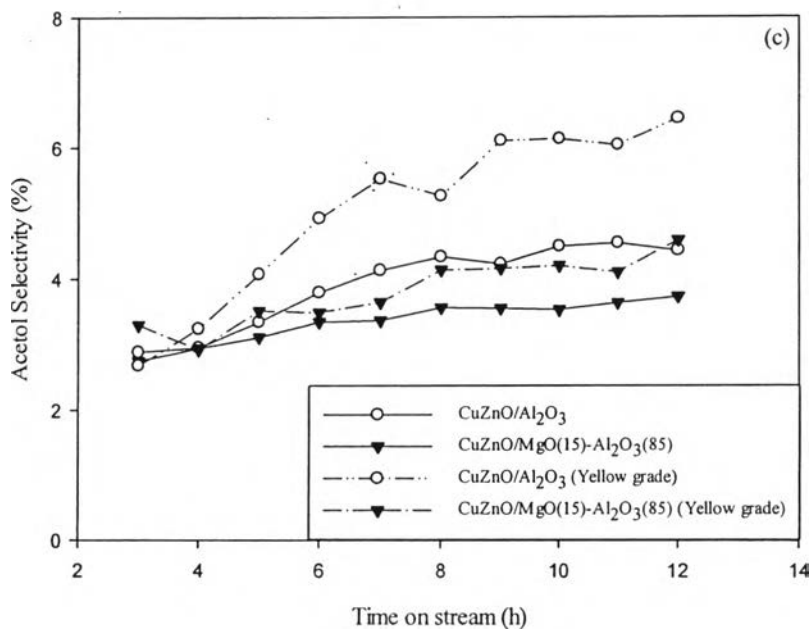


**Figure 4.7 (cont.)** Plots of (a) glycerol conversion, (b) PG selectivity, (c) acetol selectivity, and (d) EG selectivity as a function of time on stream over CuZnO/Al<sub>2</sub>O<sub>3</sub> and CuZnO/MgO(15)-Al<sub>2</sub>O<sub>3</sub>(85) catalysts in yellow grade glycerol feedstock (Reaction conditions: 80 wt.% glycerol feed, 250 °C, 500 psig, H<sub>2</sub>:glycerol = 4:1, and WHSV = 3.77 h<sup>-1</sup>)

The carbon deposited on the spent  $\text{CuZnO}/\text{Al}_2\text{O}_3$  and  $\text{CuZnO}/\text{MgO}(15)\text{-Al}_2\text{O}_3(85)$  after 12 h reaction analyzed by TPO are shown in Figure 4.8. It was found that the spent  $\text{CuZnO}/\text{Al}_2\text{O}_3$  catalyst contained the higher amount of coke (5.57 wt.%) compared to the spent  $\text{CuZnO}/\text{MgO}(15)\text{-Al}_2\text{O}_3(85)$  (3.52 wt.%). This result is consistent with the faster deactivation of  $\text{CuZnO}/\text{Al}_2\text{O}_3$  catalyst.

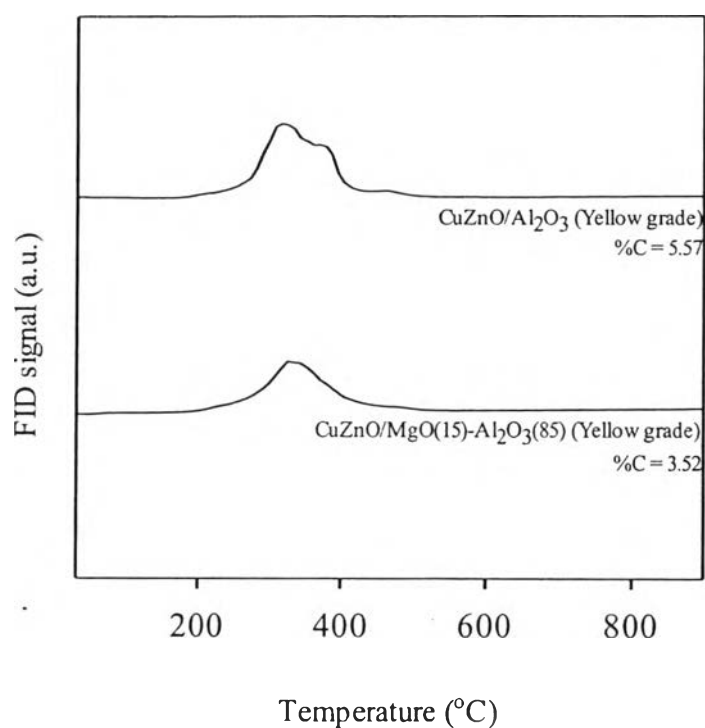


**Figure 4.8** Temperature programmed oxidation (TPO) profiles of the spent  $\text{CuZnO}/\text{Al}_2\text{O}_3$  and  $\text{CuZnO}/\text{MgO}(15)\text{-Al}_2\text{O}_3(85)$  catalysts in yellow grade glycerol feedstock after 12 h TOS. (Reaction conditions: 80 wt.% glycerol feed, 250 °C, 500 psig,  $\text{H}_2$ :glycerol = 4:1, and  $\text{WHSV} = 3.77 \text{ h}^{-1}$ ).

Fourier transform infrared spectroscopy (FTIR) was used to identify the organic compounds that adhere to catalyst surface during reaction. Figure 4.9 showed that the FTIR spectra of fresh  $\text{CuZnO}/\text{Al}_2\text{O}_3$  and  $\text{CuZnO}/\text{MgO}(15)\text{-Al}_2\text{O}_3(85)$  catalysts were quite similar. In case of spent  $\text{CuZnO}/\text{Al}_2\text{O}_3$  and  $\text{CuZnO}/\text{MgO}(15)\text{-Al}_2\text{O}_3(85)$ , FTIR profiles showed several peaks at wavenumbers of

2940, 1730, and 1380  $\text{cm}^{-1}$ . The 2940  $\text{cm}^{-1}$  peak may indicate the presence of a -CHO bond. The peak at 1730  $\text{cm}^{-1}$  may indicate the presence of a  $-\text{C}=\text{CH}_x$  bonds. Finally, 1380  $\text{cm}^{-1}$  may indicate the presence of a  $-\text{COCH}_3$  bond on the catalysts (Silvey *et al.*, 2011). For the spent CuZnO/  $\text{Al}_2\text{O}_3$ , the high intensity of FTIR spectra were clearly to showing that higher amounts of organic compounds are attaching to the surface area of the catalyst during reaction, resulted in activity loss due to blockage of active sites or pores of catalysts. This evidence confirmed that CuZnO/MgO(15)- $\text{Al}_2\text{O}_3$ (85) could resist organic compound impurities presented in yellow grade glycerol greater than CuZnO/ $\text{Al}_2\text{O}_3$ , leading to higher catalytic activity and stability.

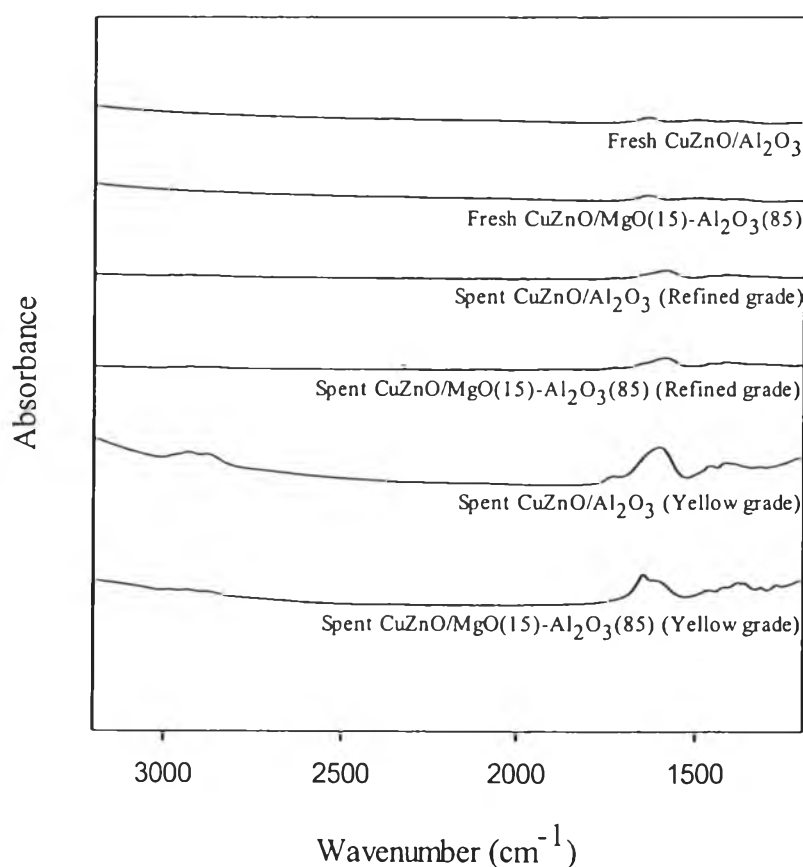


**Figure 4.9** FTIR spectra of fresh and spent CuZnO/ $\text{Al}_2\text{O}_3$  and CuZnO/MgO(15)- $\text{Al}_2\text{O}_3$ (85) catalyst in yellow grade glycerol feedstock after 12 h TOS. (Reaction conditions: 80 wt.% glycerol feed, 250 °C, 500 psig,  $\text{H}_2$ :glycerol = 4:1, and WHSV = 3.77  $\text{h}^{-1}$ ).

#### 4.2.3 Effect of Alkali (NaOH) Addition in Feedstock

As compared with yellow grade glycerol, technical grade glycerol is less expensive and more abundant. However, technical grade glycerol contains high amounts of KOH or NaOH, remained catalyst, in the biodiesel production process. These impurities might decrease the catalytic activity of the modified catalysts. Therefore, before the modified catalysts were actually applied to technical grade glycerol, the two highest performance catalysts (CuZnO/Al<sub>2</sub>O<sub>3</sub> and CuZnO/MgO(15)-Al<sub>2</sub>O<sub>3</sub>(85)) were selected to investigate the effect of 0.1% NaOH impurity contained in refined glycerol feedstock.

Figure 4.10 illustrates the plots of glycerol conversion, propylene glycol (PG) selectivity, acetol selectivity and ethylene glycol (EG) selectivity as a function of time on stream over CuZnO/Al<sub>2</sub>O<sub>3</sub> and CuZnO/MgO(15)-Al<sub>2</sub>O<sub>3</sub>(85) catalysts on NaOH impurity in glycerol feedstock—the refined glycerol and the refined glycerol mixed with 0.1% NaOH. The results showed that the glycerol conversion of both CuZnO/Al<sub>2</sub>O<sub>3</sub> and CuZnO/MgO(15)-Al<sub>2</sub>O<sub>3</sub>(85) catalysts were decreased when adding small amount of NaOH in glycerol feedstock, this might be due to Na poison the active site of catalysts. It was noticed that the catalytic activity of CuZnO/MgO(15)-Al<sub>2</sub>O<sub>3</sub>(85) remained similar with the beginning of reaction, whereas, the glycerol conversion of CuZnO/Al<sub>2</sub>O<sub>3</sub> was continuously dropped. This indicated that NaOH impurity was not affected to the reaction stability of CuZnO/MgO(15)-Al<sub>2</sub>O<sub>3</sub>(85) catalyst. Moreover, addition of alkali in glycerol feedstock improved the propylene glycol selectivity of CuZnO/MgO(15)-Al<sub>2</sub>O<sub>3</sub>(85). This might be due to the decreasing of the glycerol conversion over CuZnO/MgO(15)-Al<sub>2</sub>O<sub>3</sub>(85) led to decrease the formation of acetol, which was the intermediate product. Moreover, the hydrogenation active surface of CuZnO/MgO(15)-Al<sub>2</sub>O<sub>3</sub>(85) might less affected by NaOH impurity. Therefore, the low amounts of acetol intermediate product were completely converted to form propylene glycol, resulting in the higher propylene glycol selectivity compared to CuZnO/Al<sub>2</sub>O<sub>3</sub>. However, the ethylene glycol selectivity did not change as shown in Figure 4.10(d).

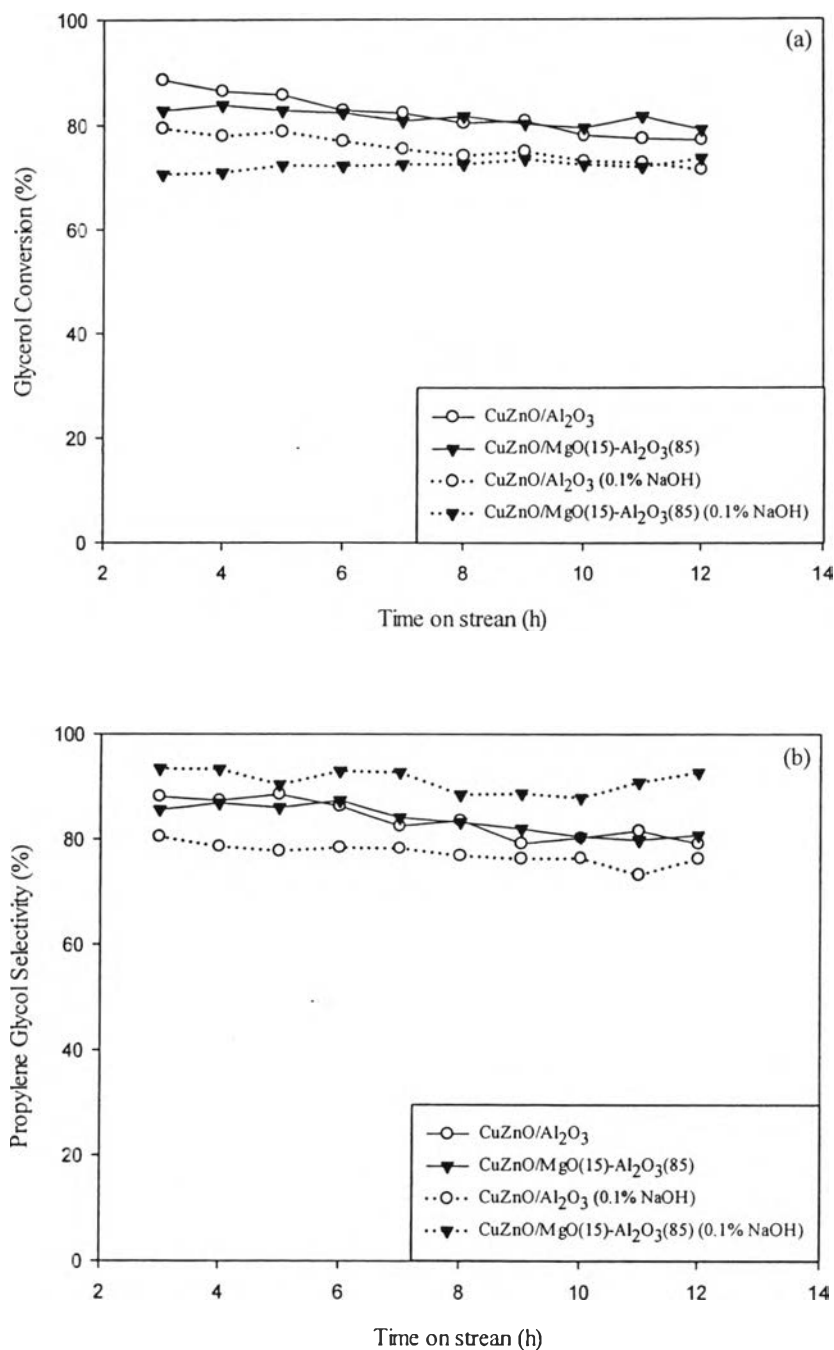


**Figure 4.10** Plots of (a) glycerol conversion, (b) PG selectivity, (c) acetol selectivity, and (d) EG selectivity as a function of time on stream over CuZnO/Al<sub>2</sub>O<sub>3</sub> and CuZnO/MgO(15)-Al<sub>2</sub>O<sub>3</sub>(85) catalysts in 0.1% NaOH dissolved in glycerol feedstock (Reaction conditions: 80 wt.% glycerol feed, 250 °C, 500 psig, H<sub>2</sub>:glycerol = 4:1, and WHSV = 3.77 h<sup>-1</sup>).

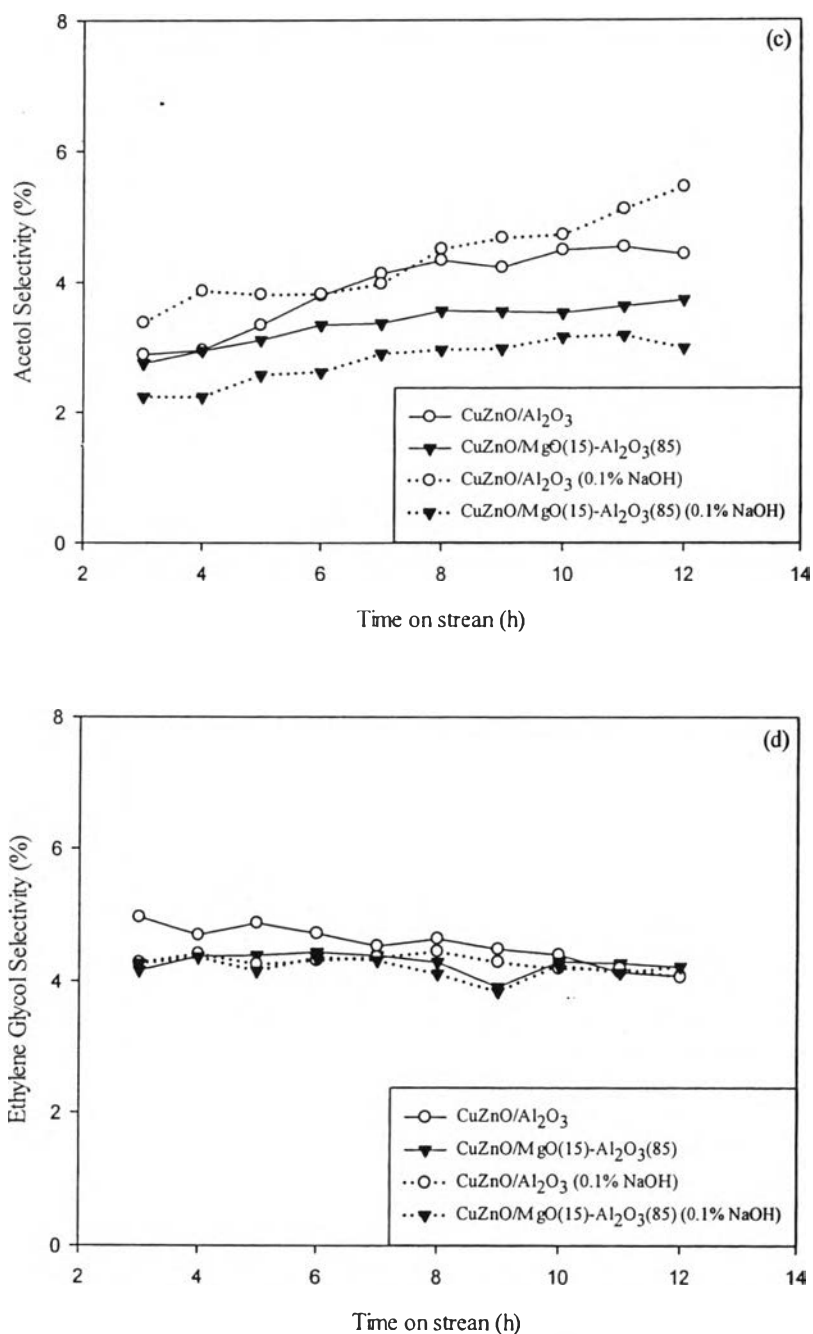


**Figure 4.10 (cont.)** Plots of (a) glycerol conversion, (b) PG selectivity, (c) acetol selectivity, and (d) EG selectivity as a function of time on stream over CuZnO/Al<sub>2</sub>O<sub>3</sub> and CuZnO/MgO(15)-Al<sub>2</sub>O<sub>3</sub>(85) catalysts in 0.1% NaOH dissolved in glycerol feedstock (Reaction conditions: 80 wt.% glycerol feed, 250 °C, 500 psig, H<sub>2</sub>:glycerol = 4:1, and WHSV = 3.77 h<sup>-1</sup>).

The TPO profiles and the amounts of carbon deposition on the spent CuZnO/Al<sub>2</sub>O<sub>3</sub> and CuZnO/MgO(15)-Al<sub>2</sub>O<sub>3</sub>(85) catalysts are shown in Figure 4.11. The results showed that by using the refined glycerol as feedstock, the spent catalysts contained lower amount of coke compared to the refined glycerol mixed with 0.1% NaOH. Noticeably, amounts of coke deposition on the spent CuZnO/Al<sub>2</sub>O<sub>3</sub> catalyst was higher than CuZnO/MgO(15)-Al<sub>2</sub>O<sub>3</sub>(85). This result was confirmed that interaction between metal and mixed oxide support could play a role in the coke formation on the catalyst.

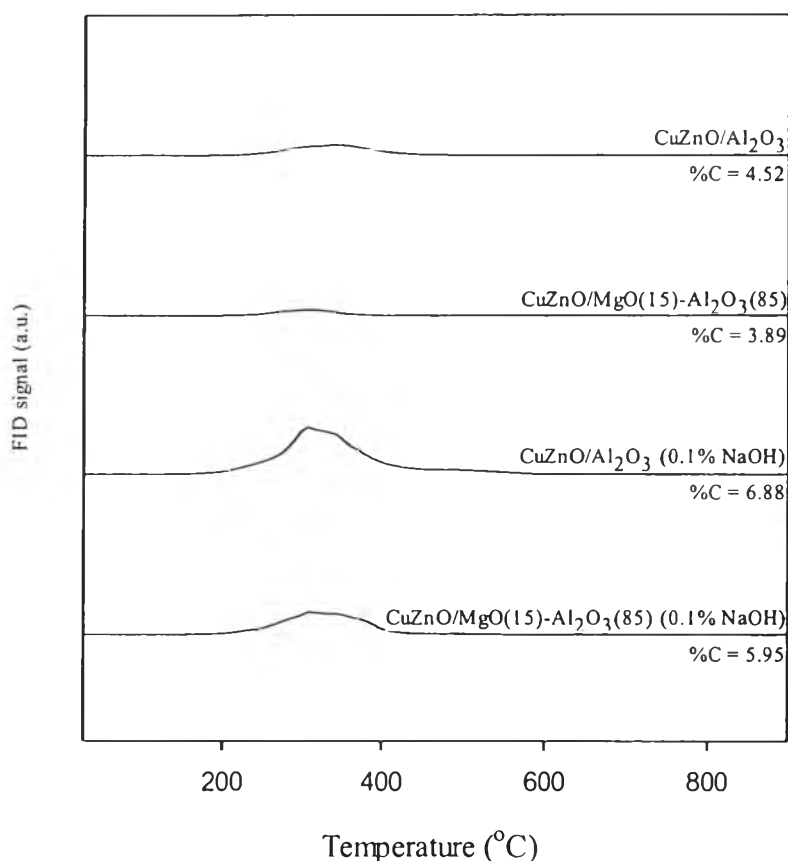


**Figure 4.11** Temperature programmed oxidation (TPO) profiles of the spent CuZnO/Al<sub>2</sub>O<sub>3</sub> and CuZnO/MgO(15)-Al<sub>2</sub>O<sub>3</sub>(85) catalysts in 0.1% NaOH dissolved in glycerol feedstock after 12 h TOS. (Reaction conditions: 80 wt.% glycerol feed, 250 °C, 500 psig, H<sub>2</sub>:glycerol = 4:1, and WHSV = 3.77 h<sup>-1</sup>).

Atomic absorption spectroscopy (AAS) was applied to determine the amount of alkali deposited on the spent CuZnO/Al<sub>2</sub>O<sub>3</sub> and CuZnO/MgO(15)-Al<sub>2</sub>O<sub>3</sub>(85) catalysts. Table 4.4 shows that Na was deposited on CuZnO/Al<sub>2</sub>O<sub>3</sub> but hardly deposited on CuZnO/MgO(15)-Al<sub>2</sub>O<sub>3</sub>(85). This could be because Na is a basic metal and Al<sub>2</sub>O<sub>3</sub> containing in the mixed oxide support is an acid metal oxide. Therefore, Na would attach much stronger bond with the surface of CuZnO/Al<sub>2</sub>O<sub>3</sub> than CuZnO/MgO(15)-Al<sub>2</sub>O<sub>3</sub>(85).

**Table 4.4** Concentrations of alkali in feedstock and the spent CuZnO/Al<sub>2</sub>O<sub>3</sub> and CuZnO/MgO catalysts analyzed by AAS

Catalyst	Alkali concentrations	
	Feedstock (ppm)	Spent Catalyst (ppm)
CuZnO/Al <sub>2</sub> O <sub>3</sub>	1,042	104.17
CuZnO/MgO(15)-Al <sub>2</sub> O <sub>3</sub> (85)	1,084	19.98